Diffusing Polymers in Confined Microdomains and Estimation of Chromosomal Territory Sizes from Chromosome Capture Data

A. Amitai and D. Holcman

Group of Applied Mathematics and Computational Biology, Ecole Normale Supérieure, 46 rue d'Ulm 75005 Paris, France

(Received 19 March 2013; published 14 June 2013)

Is it possible to extract the size and structure of chromosomal territories (confined domain) from the encounter frequencies of chromosomal loci? To answer this question, we estimate the mean time for two monomers located on the same polymer to encounter, which we call the mean first encounter time in a confined microdomain (MFETC). We approximate the confined domain geometry by a harmonic potential well and obtain an asymptotic expression that agrees with Brownian simulations for the MFETC as a function of the polymer length, the radius of the confined domain, and the activation distance radius ε at which the two searching monomers meet. We illustrate the present approach using chromosome capture data for the encounter rate distribution of two loci depending on their distances along the DNA. We estimate the domain size that restricts the motion of one of these loci for chromosome II in yeast.

DOI: 10.1103/PhysRevLett.110.248105 PACS numbers: 87.16.Sr, 02.50.Fz, 05.40.−a, 82.20.Uv

Chromosome capture is a method where high-throughput data are generated about an instant of nuclear chromosomal organization [1,2]. These data consist of a collection of DNA fragments of various sizes, and the frequency of each fragment is a measure of the proximity of two DNA loci. It should be possible in principle to reconstruct the local chromosomal organization from this data. Yet such reconstruction remains a daunting challenge.

We propose here to develop a method based on a polymer model to estimate the size of a chromosomal domain from the distribution of encounter frequency of a loci with others, obtained from chromosome capture data. Indeed, the frequency that two loci encounter is the rate at which two monomers of a polymer chain meet. This rate is the reciprocal of the mean first passage time $\langle \tau_e \rangle$, which we call the mean first encounter time in confined domain (MFETC). We will derive an approximated expression for $\langle \tau_e \rangle$ using the Rouse polymer model [3] in a ball of radius A, where the polymer length is N and the radius ε is the distance at which the two monomers meet [Fig. 1(a)]. By fitting empirical data of chromosome capture, we will obtain the radius of chromosomal confined domain.

Although polymer looping time in a free space was previously analyzed using numerical and asymptotic methods [4–11] and experimental methods [12,13], these studies cannot be used here directly. Thus, we consider here the encounter between monomers in a confined domain. In addition, although the persistence length of the chromatin fiber was previously estimated to be 200 nm [14], new *in vivo* experimental evidence suggests that it is only of the order of tens of nms [15]. We shall thus neglect the bending elastic in a first approximation and develop an approach based on Rouse polymer.

The stochastic description of a Rouse polymer is a collection of monomers positioned at $\boldsymbol{R}_n$ $(n=1,2,\ldots,N)$, moving with a random Brownian motion coupled to a spring force originating from the nearest neighbors,

$$\phi(\boldsymbol{R}_1,\ldots,\boldsymbol{R}_N)_{\text{Rouse}} = \frac{\kappa}{2}\sum_{n=1}^{N}(\boldsymbol{R}_n - \boldsymbol{R}_{n-1})^2, \qquad (1)$$

where the spring constant $\kappa = 3k_BT/b^2$ is related to the standard deviation b of the distance between adjacent monomers [3] with k_B the Boltzmann coefficient and T the temperature. In units of k_BT, we have $\kappa = 3/b^2$ and $D = 1/\gamma$, where γ is the friction coefficient. In the Smoluchowski's limit of the Langevin equation [16], the dynamics of monomer $\boldsymbol{R}_n$ is

$$\frac{d\boldsymbol{R}_n}{dt} = -D\nabla_{\boldsymbol{R}_n}\phi_{\text{Rouse}} + \sqrt{2D}\frac{d\boldsymbol{w}_n}{dt}, \qquad (2)$$

for $n = 1,\ldots,N$ and each $\boldsymbol{w}_n$ is an independent three-dimensional white Gaussian noise with mean zero and variance 1.

The MFETC $\langle \tau_e \rangle$ is the mean time for the two ends $\boldsymbol{R}_N, \boldsymbol{R}_1$ to come to a distance $\varepsilon < b$, when the polymer evolves inside a confining three-dimensional ball of radius A. To obtain an asymptotic computation for the time $\langle \tau_e \rangle$, we will replace the boundary on the polymer dynamics by a field of force [Fig. 1(b)], thus changing the potential ϕ_{Rouse} in Eq. (2) by

$$\phi_h = \phi_{\text{Rouse}} + \frac{\beta}{2}\sum_{n=1}^{N}\boldsymbol{R}_n^2 = \frac{1}{2}\sum_{p=0}^{N-1}(\kappa_p + \beta)\boldsymbol{u}_p^2, \qquad (3)$$

where $\kappa_p = 4\kappa\sin^2(p\pi/2N)$, $\boldsymbol{u}_p$ are the coordinates in which ϕ_{Rouse} [3] is diagonal, and the strength β is a free parameter that will be adjusted to account for confinement [17]. Our first result which approximates the MFETC is the new asymptotic formula for the mean time $\langle \tau_h \rangle$ that the two end monomers of a Rouse polymer moving in a harmonic potential meet. For $\varepsilon \ll b$, it is

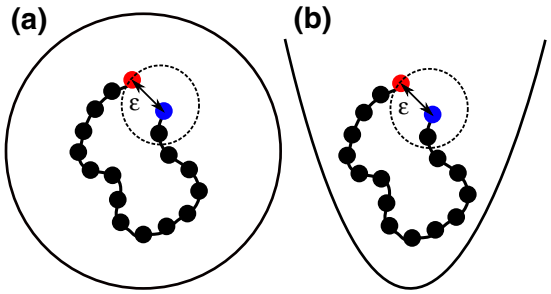

FIG. 1 (color online). MFETC of polymer ends in a confined domain and in a potential well. (a), (b) Schematic representation of the encounter process between the ends of a polymer in a confined ball and in a harmonic potential.

$$\langle \tau_h \rangle \approx \frac{2^{1/2}}{4\pi\varepsilon D}\left[\frac{4\pi N}{N^2\beta + \pi^2\kappa} + \frac{4}{\sqrt{\kappa\beta}} \times \left[\frac{\pi}{2} - \tan^{-1}\left(2\sqrt{\kappa/\beta}\tan(\pi/2N)\right)\right]\right]^{3/2} + \mathcal{O}(1). \tag{4}$$

In contrast to all previous formulas obtained for free looping polymer [6–11,18] [Fig. 2(d)], when N is large, $\langle \tau_h \rangle$ does not diverge to infinity, but converges to an asymptotic value $(1/\pi\varepsilon D)(\pi/\sqrt{\kappa\beta})^{3/2}$. The criteria to choose the potential strength β is that the root mean square end-to-end distance of the polymer in the potential field is equal to the square radius of the confining ball domain A, that is

$$\langle (\boldsymbol{R}_N(\beta) - \boldsymbol{R}_1(\beta))^2 \rangle = A^2 \quad \text{for } N \gg 1. \tag{5}$$

This equation can be solved explicitly using the averaging over the Boltzmann distribution $e^{-\phi_h}dx$ and we obtain

$$\beta = \frac{12}{A^4/b^2 + 2A^2}. \tag{6}$$

The looping time for a polymer in a confined domain.—We shall now explain how we extended the methodology developed for the looping of a free polymer [11] to derive formula (4). We describe the dynamics of a polymer in confined domain by Eq. (2) with the harmonic potential well. The MFETC $\langle \tau_h \rangle$ is computed from the relation

$$\langle \tau_h \rangle \approx \frac{1}{D\lambda_0^\epsilon}, \tag{7}$$

where λ_0^ϵ is the first eigenvalue of the operator $\mathcal{L}$,

$$\mathcal{L}p = \frac{D}{N}(\Delta_{u_0} p(\boldsymbol{u}) + \nabla_{u_0}(\nabla_{u_0}\phi_h p(\boldsymbol{u}))) + \sum_{k=1}^{N-1} D\Delta_{u_k} p(\boldsymbol{u}) + D\nabla_{u_k}(\nabla_{u_k p}\phi_h p(\boldsymbol{u})), \tag{8}$$

where $\boldsymbol{u} = (\boldsymbol{u}_0, \ldots, \boldsymbol{u}_{N-1}) \in \Omega = \mathbb{R}^{3N}$ and the absorbing boundary condition is $p(\boldsymbol{u}) = 0$ for $\boldsymbol{u} \in \partial S_\epsilon$, where S_ϵ is the closed polymer configuration space,

$$S_\epsilon = \left\{\boldsymbol{u} \in \Omega \text{ s.t. } \sum_{p \text{ odd}} \boldsymbol{u}_p \cos(p\pi/2N) \le \frac{\varepsilon}{2}\right\}. \tag{9}$$

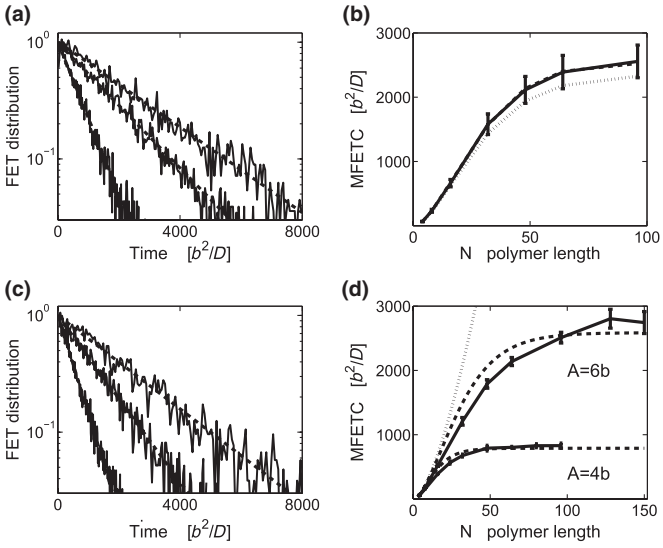

FIG. 2. The encounter of the end monomers for confined Rouse polymer. (a) First encounter time distributions for a Rouse polymer confined in a harmonic well for various polymer lengths $N = 16, 32, 64$ (left to right) with $\beta = 0.01b^{-2}$ and $\varepsilon = 0.01b$. Note that one exponential (dashed line) is enough to describe the process. (b) Brownian simulations (full line) are compared to the MFETC computed [Eqs. (7) and (11)] by taking the first order only in ε (pointed line) and by taking into account the second-order correction (dashed line) given by Eq. (18). Fitting the parameter γ to our simulation results gave $\tilde{\gamma} = 10$. (c) First encounter time distributions for a polymer in a ball of radius $A = 6b$, for various polymer lengths ($N = 16, 32, 64$ left to right). A single exponential (dashed line) is sufficient to approximate the distribution over the entire range. (d) MFETC as a function of the polymer length: Brownian simulations (full lines) in spheres of radii $A = 4b, 6b$ with $\varepsilon = 0.01b$. We estimate the MFETC (dashed lines) using the harmonics well approximation [Eq. (7) with Eq. (11)], where β was fitted to the simulation results $\beta_4 = 0.0406b^{-2}$, $\beta_6 = 0.0089b^{-2}$. The MFET is also shown (points) for a freely moving polymer (Eq. (2) [11]).

To compute the eigenvalue, we use the perturbation formula [19]

$$\lambda_0^\epsilon = \lambda_0^0 + 4\pi\epsilon \int_{S_0} w_{\lambda_0^0}^2 dV_x, \tag{10}$$

where $w_{\lambda_0^0} = |\mathbb{R}^{3N}|_{\phi_h}^{-1/2}$ is the eigenfunction associated with λ_0^0 for the volume $dV_x = e^{-\phi_h}d\mathbf{x}_g$, and $d\mathbf{x}_g$ is the Euclidean measure over S_0 [obtained by taking $\varepsilon = 0$ in Eq. (9)]. With $\lambda_0^0 = 0$ and a direct computation, we obtain that

$$\lambda_0^\epsilon = 4\pi\epsilon(2\pi)^{-3/2}\left[\frac{\sum_{p \text{ odd}} \omega_p^2}{K(N,\beta)}\right]^{3/2} + \mathcal{O}(\epsilon^2), \tag{11}$$

where $\omega_p = \cos(p\pi/2N)$ and

$$K(N,\beta) = \sum_{p \text{ odd}} \frac{\omega_p^2}{\kappa_p + \beta}. \tag{12}$$

Thus for $N \gg 1$, using relation (7), an asymptotic expansion gives formula (4).

Second-order expansion of λ_0^ϵ in ϵ.—The effect of the boundary is seen in the second-order term of the expansion of λ_0^ϵ as a function of ϵ [20],

$$\lambda_0^\epsilon \sim 4\pi\lambda_1^0\epsilon + (4\pi)^2\lambda_2^0\epsilon^2 + \mathcal{O}(\epsilon^3), \tag{13}$$

with $\lambda_2^0 = \tilde{\gamma}\int_{S_0}\int_{S_0} G(\boldsymbol{x};\boldsymbol{y})dV_x dV_y$, where $\tilde{\gamma}$ is a constant, G is the Green's function associated to the operator $\mathcal{L}$. It can be computed in terms of the unperturbed eigenfunctions ($w_{\lambda_i^0}$) and eigenvalues (λ_i) by

$$G(\boldsymbol{x};\boldsymbol{y}) = -\sum_{i\neq 0}\frac{w_{\lambda_i^0}(\boldsymbol{x})w_{\lambda_i^0}(\boldsymbol{y})}{\lambda_i}. \tag{14}$$

We will use the following approximation:

$$\lambda_2^0 = -\tilde{\gamma}\sum_{k\neq 0}\frac{\langle w_{\lambda_k^0}|w_{\lambda_0^0}\rangle_{S_0}^2}{\lambda_k} \approx -\tilde{\gamma}\frac{\langle w_{\lambda_2^0}|w_{\lambda_0^0}\rangle_{S_0}^2}{\lambda_2}, \tag{15}$$

where

$$\langle w_{\lambda_i^0}|w_{\lambda_0^0}\rangle_S = \int_{S_0} e^{-\phi_h(\boldsymbol{u})}w_{\lambda_i^0}(\boldsymbol{u})w_{\lambda_0^0}(\boldsymbol{u})dV_g. \tag{16}$$

Since the first nonzero eigenfunction ($w_{\lambda_{1,i}^0}$) is linear with $u_{1,i}$, the scalar product is zero and we approximate (15) by computing the product associated with the second eigenvalue of $p = 1$ in one of the spatial directions i. The eigenfunction is given by the second Hermite polynomial,

$$w_{\lambda_{2,i}^0} = (2|\mathbb{R}^{3N}|_{\phi_h})^{-1/2}((\kappa_1+\beta)(u_{1,i})^2 - 1). \tag{17}$$

In summary, we obtain that

$$\lambda_0^\epsilon = \frac{\varepsilon}{8\pi^{1/2}}\left[\frac{N}{K(N,\beta)}\right]^{3/2} - \frac{2^{-8}\pi^{-1}\varepsilon^2\tilde{\gamma}N^3}{(\kappa_1+\beta)^3K(N,\beta)^5}. \tag{18}$$

For large N, $K(N,\beta)\approx N/4\sqrt{\kappa\beta}$ and $\kappa_1 = 4\kappa\sin^2(\pi/2N)$. Finally, using (7) for small ε and fixed N, we obtain a refined approximation compared to (4) for the MFETC,

$$\langle\tau_\epsilon\rangle \approx \frac{2^3\pi^{1/2}}{D\varepsilon}\left[\frac{K(N,\beta)}{N}\right]^{3/2} + \frac{\tilde{\gamma}(16\kappa\sin^2(\pi/2N)+\beta)^{-3}}{DK(N,\beta)^2}.$$

Contrary to the looping time in free space, where $\langle\tau_\epsilon\rangle = a_1N^{3/2}/\varepsilon + a_2N^2$ [11] (a_1, a_2 are constants) for $N \gg 1$, where the N^2 term dominates, in the confined case, only the first term is increasing with the length N. Indeed, for a confined polymer, the two ends are bounded by the diameter of the domain.

To validate the Poissonian nature of looping in confined domain, we further investigated the survival probability $P(t)$ that a loop is not formed before time t. The first encounter time (FET) distribution $p(t)$ is the derivative of P and can be obtained by expanding the probability density function solution of $(\partial p/\partial t) = \mathcal{L}(p)$ using an eigenfunction expansion

$$p(t) = \sum_{i=0}^{\infty} C_i e^{-\lambda_i^\epsilon Dt} \approx e^{-\lambda_0^\epsilon Dt}, \tag{19}$$

where C_i are coefficients. Using Brownian simulations, we obtained the FET of the two ends of a polymer in a harmonic well [Fig. 2(a)]. Interestingly, unlike the FET distribution for a free polymer, $p(t)$ is well approximated by a single exponential, even for long polymers, showing that the higher exponential terms [Eq. (19)] do not contribute. We conclude that the encounter time for a polymer in a harmonic well is Poissonian. Moreover, as observed from matching of the theoretical formula (4) and Brownian simulations for the MFETC in a potential well [Fig. 2(b)], the first-order correction in ε is a very satisfactory and stable approximation even for large N and small ε.

Brownian simulations of polymer looping in a confined domain.—To validate formula (4) for a polymer looping in a confined domain, we used Brownian simulations of a Rouse polymer in confining spheres [Fig. 2(d)] of different radii and first compared it with the formula in a free domain. Although for small polymer lengths, there is almost no difference between confined and nonconfined looping time, for long polymers, the MFETC reaches an asymptotic value, which depends on the radius of the domain. Interestingly, when the interacting monomers are not at the ends of a polymer chain, the MFETC is reduced in a range between 5% and 30% [26], due to the interaction of the additional monomers with the boundary [17]. Finally, the distribution of arrival time [Fig. 2(c)] for short and long polymers can be approximated by a single exponential, confirming that the looping event is almost Poissonian. This is in contrast with looping in the bulk, where for longer polymers, a second exponential is necessary. We compared the MFETC as computed from Eq. (7), taking only the first order in ε [Eq. (11)], where the potential strength β was fitted to the Brownian simulation. The calibration formula (6) gives very similar values to the fitted ones. For $A = 4b$, $6b$, the fitted values are $\beta_{\text{fit},4} = 0.0406b^{-2}$, $\beta_{\text{fit},6} = 0.0089b^{-2}$, respectively, while the calibration formula (6) gives $\beta_{\text{cal},4} = 0.0417b^{-2}$, $\beta_{\text{cal},6} = 0.0088b^{-2}$. We conclude that using the fitting procedure (6), it is possible to access the radius of the confined sphere.

DNA looping inside nuclear territories and analysis of chromosome capture data.—The mean first encounter time or looping time of a Rouse polymer in a confined domain increases with the polymer length to an asymptotic value, which depends on the size of the confined domain. We now estimate the mean encounter time for a chromosomal locus to find another one inside the convex envelope of the chromosome, also called chromosome territory [21] [Fig. 3(a). This territory results from the self-avoiding interactions with other chromosomes. Consequently, a chromosome cannot penetrate the territory of another one [22]. Inside a territory, the MFETC between two loci increases with

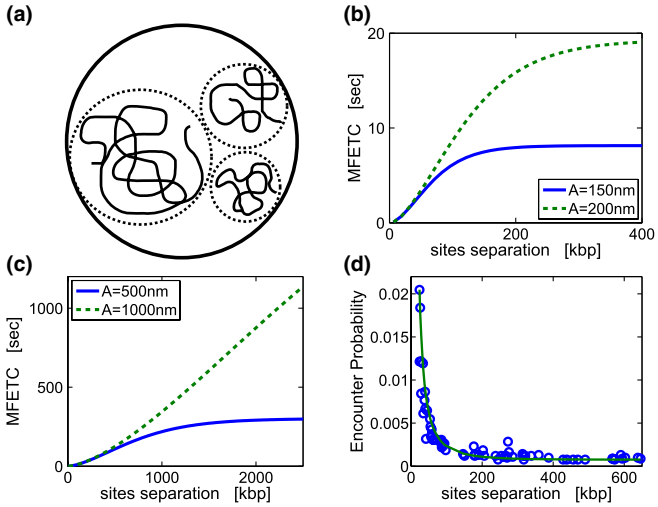

FIG. 3 (color online). Encounter between two DNA loci inside a domain. (a) Schematics representation of chromosome territories inside the nucleus. Chromosome are naturally separated due to self-avoiding interactions. (b), (c) MFETC of two sites located on the same chromosome as a function of their separation along the DNA strand. Chromosomes are confined in domains of radii $A = 150$, 200, 500, 1000 nm. The encounter radius is $\varepsilon = 5$ nm. (d) Encounter probability of a locus on chromosome II in the yeast and fitting of our looping probability formula. The effective confining radius extracted using our calibration formula is $A = 230$ nm.

their distance along the strand [Fig. 3(b) and 3(c)] and depends on the size of the confinement. We model the chromatin fiber as a Rouse chain composed of N monomers and choose the standard deviation of the bond length to be $b = 30$ nm, representing the 30-nm fiber, and neglect the strand-bending elasticity. Each monomer represents 3.2 kbps along the chromosome [23], and the diffusion coefficient of a monomer is $D = 10 \times 10^3$ nm^2/ sec [24]. We choose an absorbing radius of $\varepsilon = 5$ nm. Using formula (7) and taking only the first-order term in ε [Eq. (11)] and the calibration formula (6) for the strength of the confining potential, we found that the MFETC strongly depends on the confinement radius (chromosome territories) and can vary between 8 sec for a small domain of radius $A = 150$ nm to about 5 min for a large domain of radius $A = 500$ nm. We will now show that we can use this approach to extract the effective confinement radius from measured looping distribution. The four dimensional capture (4C) method identifies chromosomal interactions genome wide by coupling chromosome conformation capture-on-chip. This method captures chromosome conformation *in vivo* by ligating close loci together. One example is the 4C data set of the yeast *Saccharomyces cerevisiae* [2]. The method reveals the encounter probabilities between chromosomal sites at steady state. The frequency of encounter is inversely proportional to the MFETC; thus, the encounter frequency can be obtained from the MFETC formula. Interestingly, although the MFETC can vary depending on the position along the polymer chain of the monomers that will encounter, the normalized rate (the reciprocal of the MFETC divided by its integral over the length) of monomer interaction (as experimentally measured) is first independent on the encounter rate radius ε (as it cancels out in the normalization). Second, the encounter probability depends only on the distance between two monomer pairs along the chain and is in fact not much affected by the remaining polymer tails located beyond them [26].

Chromatin can be organized in higher-order structure such as stable separated blobs that result from local specific interactions. The current stage of the analysis model does not take into account the effects due to these higher-order structures in the chromosome. Another limitation of the present model when applied to yeast is due to the Rabl chromosomal configuration where the centromeres are connected to the mitotic spindle body. Indeed, this interaction breaks the radial symmetry. Thus, by choosing a locus distant from the centromere, we shall overcome this difficulty. Based on these considerations, we now apply the above approach to 4C data in yeast, where higher-order structures are not dominant. We remark that the radius of the yeast nucleus is fairly small (1 μm) and the confinement effect is not related to the chromosome territories but is certainly due to some interaction with the nuclear membrane. We used the encounter probability data [2] for the locus at position 99 kbp from the right end of chromosome II in the yeast [Fig. 3(d)] and fitted them with the encounter formula [Eqs. (7) and (11)], where β is the only free parameter. We found that $\beta = 3.91 \times 10^{-6}$ nm^{-2}. Using formula (6), we obtain an effective confinement radius of $A = 230$ nm, representing a subdomain of the yeast nucleus [25]. Moreover, as predicted by our model, for large distances along the strand, the encounter probability reaches an asymptotic value rather than going asymptotically to zero [Fig. 3(d)]. This shows that the encounter of loci pair is affected by nuclear confinement.

An extension of the present polymer model beyond the Rouse linear chain would be important to account for higher-order organization of the chromosome. Finally, geometrical constraints of chromatin loci are classically obtained by single-particle tracking of a fluorescent spot on the chromatin. Extracting spatial information from chromosome capture data, which can later be compared to single-particle tracking experiment, is now possible. In this way, results of those two very different methods can be compared.

[1] E. Lieberman-Aiden, N. L. van Berkum, L. Williams, M. Imakaev, T. Ragoczy, A. Telling, I. Amit, B. R. Lajoie, P. J. Sabo, M. O. Dorschner, R. Sandstrom, B. Bernstein, M. A. Bender, M. Groudine, A. Gnirke, J. Stamatoyannopoulos,

L. A. Mirny, E. S. Lander, and J. Dekker, Science **326**, 289 (2009).
[2] Z. Duan, M. Andronescu, K. Schutz, S. McIlwain, Y. J. Kim, C. Lee, J. Shendure, S. Fields, C. A. Blau, and W. S. Noble, Nature (London) **465**, 363 (2010).
[3] M. Doi and S. F. Edwards, *The Theory of Polymer Dynamics* (Clarendon Press, Oxford, 1986).
[4] G. Wilemski and M. Fixman, J. Chem. Phys. **60**, 878 (1974).
[5] A. Szabo, K. Schulten, and Z. Schulten, J. Chem. Phys. **72**, 4350 (1980).
[6] R. W. Pastor, R. Zwanzig, and A. Szabo, J. Chem. Phys. **105**, 3878 (1996).
[7] B. A. Friedman and C. Yeung, Eur. Phys. J. E **21**, 25 (2006).
[8] N. M. Toan, G. Morrison, C. Hyeon, and D. Thirumalai, J. Phys. Chem. B **112**, 6094 (2008).
[9] J. Z. Y. Chen, H.-K. Tsao, and Y.-J. Sheng, Phys. Rev. E **72**, 031804 (2005).
[10] C. Ting, J. Ding, and J. Z. Y. Chen, Macromolecules **39**, 5540 (2006).
[11] A. Amitai, I. Kupka, and D. Holcman, Phys. Rev. Lett. **109**, 108302 (2012).
[12] L. Ringrose, S. Chabanis, O. P. Angrand, C. Woodroofe, and A. F. Stewart, EMBO J. **18**, 6630 (1999).
[13] J. Allemand, S. Cocco, N. Douarche, and G. Lia, Eur. Phys. J. E **19**, 293 (2006).
[14] K. Bystricky, P. Heun, L. Gehlen, J. Langowski, and S. M. Gasser, Proc. Natl. Acad. Sci. U.S.A. **10147**, 16495 (2004).
[15] A. Bancaud, GDR, Paris (private communication).
[16] Z. Schuss, *Theory and Applications of Stochastic Differential Equations* (Wiley, New York, 1980).
[17] A. Amitai, C. Amoruso, A. Ziskind, and D. Holcman, J. Chem. Phys. **137**, 244906 (2012).
[18] I. M. Sokolov, Phys. Rev. Lett. **90**, 080601 (2003).
[19] I. Chavel and E. A. Feldman, Duke Math. J. **56**, 399 (1988).
[20] A. F. Cheviakov and M. J. Ward, Math. Comput. Modell. **53**, 1394 (2011).
[21] T. Cremer and C. Cremer, Nat. Rev. Genet. **2**, 292 (2001).
[22] M. Fritsche, L. G. Reinholdt, M. Lessard, M. A. Handel, J. Bewersdorf, and D. W. Heermann, PLoS ONE **7**, e36282 (2012).
[23] H. Tjong, K. Gong, and F. Alber, Genome Res. **22**, 1295 (2012).
[24] K. Dubrana, CEA, France (private communication)
[25] P. Therizols, T. Duong, B. Dujon, C. Zimmer, and E. Fabre, Proc. Natl. Acad. Sci. U.S.A. **107**, 2025 (2010).
[26] See Supplemental Material at http://link.aps.org/supplemental/10.1103/PhysRevLett.110.248105 for MFETC and encounter probability of internal monomers compared to the end monomers.